Aerosol Climate Forcing (ACliF) Projects

ARFI, ICARB, RAWEX & NOBLE

Proceedings of the Project Review Meeting

8-9 January 2014

Space Physics Laboratory
Vikram Sarabhai Space Centre, Indian Space Research Organisation
Thiruvananthapuram - 695 022, India

GEOSPHERE BIOSPHERE PROGRAM

Inter-annual variability of aerosol over Goa, along the west coast of India – study performed during a three year period between 2008 and 2010

Shilpa Shriodkar and Harilal B.Menon
Department of Marine Sciences, Goa University, University, Goa- 403 206, India

Aerosols influence climate directly by affecting the radiative balance of the earth and indirectly by changing the cloud microphysical properties (Charlson et al., 1992). Natural source of aerosol in the atmosphere are sea salt, volcanic aerosol, biogenic aerosol and desert dust while anthropogenic sources are biomass burning and combustion of fossil fuel. Thus, depending upon their source, size and formation process, aerosols exhibit a large variability on a global scale. Typically, size distribution is bimodal constituting of fine mode aerosols of anthropogenic origin and naturally produced coarse mode aerosols (Eck et al., 1999). Thus, large spatial and temporal variability of aerosol concentration with short residence time hinder the understanding of radiative effects on Earth's radiation budget (IPCC, 2007).

Radiative properties of aerosols (single scattering albedo, ω and phase function, g) and the Ångström parameters (α, β) are influenced significantly by spectral dependence of aerosols. Such a characterization is useful tool for identifying the aerosol source region and their evolution; moreover it is also significant in modeling the radiative effect of aerosols, retrieval of aerosol parameter by remote sensing technique and applying atmospheric correction for oceanographic studies for optical remote sensing (Eck et al., 1999). The wavelength dependence of aerosol varies depending upon physical and chemical properties of aerosol and Ångström wavelength exponent (α) is commonly used to quantify this spectral dependence.

The Ångström wavelength exponent is related to Junge or power law size distribution (Junge, 1955). However, size distribution of aerosol typically does not follow the Junge distribution. Departure from these conditions often introduces curvature in the ln AOD and ln λ relationship, hence a second order polynomial fit is introduced to account for this curvature.

Identification of aerosol type by investigating the curvature spectra has gained significant importance during recent studies of aerosol over Indian subcontinent (e.g., Singh et al., 2004; Madhavan et al., 2008; Beegum et al., 2009;Kedia et al., 2011; Gularia et al., 2012). Apart from this, extensive investigations on curvature assessment have been carried out over the Northern India Ocean in the recent past (kedia et al., 2009; Kalapureddy et al., 2009; Kaskaoutis et al., 2010, 2011).

Under the ageis of aerosol radiative forcing (ARFI), continuous observations of aerosol optical depth and samplings were performed at different stations across India. In Goa, the measurements were initiated since December 2007. The report explains the microphysical characteristics of aerosol during the year 2008, 2009 and 2010.

The seasonal variability of AOD and Ångström parameters, wherein variation of α in short and long wavelength regions has been analysed in conjunction with second order Angstrom exponent $\acute{\alpha}$ and coefficients of the second order polynomial fit $a1$ and $a2$ have been probed to look for possible aerosol dominant type.

2.1. Study area and general meteorology

Goa is a tiny state along the west coast of India, surrounded by Arabian Sea at the west and Western Ghats at the east (Fig.1a). June to September demarcates south-west monsoon while December to March constitute north-east monsoon over this region. The period April May and October November represent the transition between the seasons. Thus, the study site experiences four distinct seasons, namely winter monsoon (December, January, February and March, WMS); spring inter-monsoon (April and May, SIMS); summer monsoon (June, July, August and September; SMS) and fall inter-monsoon (October and November; FIMS).The sampling site is located at Goa university campus (15.460N and 73.830E), which is ~0.7 kms from Arabian Sea and ~5 kms from capital city Panjim. Being a coastal location, land-sea breeze is a local

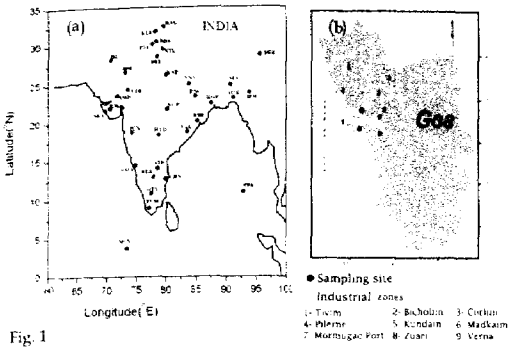

Fig. 1

Fig.1 (a) Network of stations under the Aerosol Radiative Forcing over India (ARFI) project (b) ARFI station at Goa, different industrial zones are shown as numbers from 1 to 9.

phenomenon within the boundary layer. Several industrial sites are located in the proximity of the sampling site and closest among all is the Murmagao port (Fig. 1b). Ore produced as an outcome of mining, which is a significant activity in Goa, is transported to Murmagao port mainly through Mandovi and Zuari rivers.

2.2. In-situ measurements

2.2.1. Meteorological factors

Aerosol spatial and temporal variability are governed by meteorological factors and the parameters were measured using automatic weather station (AWS). Rainfall data for the study period was obtained from Indian meteorological department situated ~4 kms from the study site. Seasonal mean variation of the meteorological factors is shown in Table 1. Wind speed increased from 1.09 m/s in WMS to 1.37 m/s in SIMS and attaining a peak of 2.10 m/s during SMS, further it reduces to 1 m/s during FIMS. It is observed that winds are mostly south/ southeasterly during WMS and southwesterly during SIMS. During SMS, wind direction changes entirely to westerly which attains southeasterly during FIMS. Relative humidity shows an increasing trend from WMS till SMS, thereafter decreases as FIMS approaches. SMS receives above normal rainfall over the study region where rainfall of 725 mm is recorded. Considerable amount of precipitation is also seen during FIMS (161mm), which is a transition phase. Rainfall during April/May constitutes to a seasonal mean of 30 mm of precipitation. Negligible amount of precipitation is noticed in December during WMS (~17 mm).

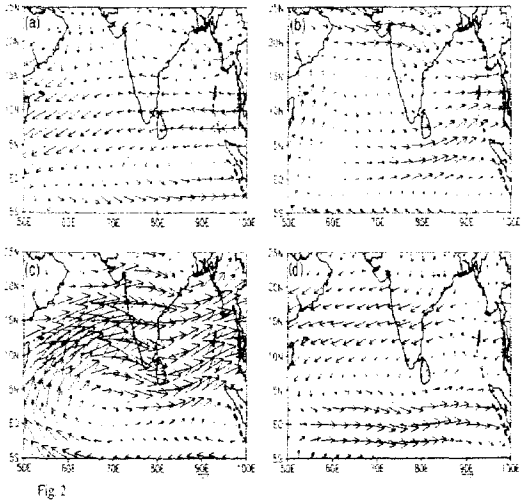

Fig 2

Fig.2. Synoptic wind (m/s at 850 hPa) over India during (a) WMS (b) SIMS (c) SMS and (d) FIMS.

Synoptic wind at surface (850 hPa), using National Center for Prediction (NCEP) data, revealed that during WMS, winds are moderate and easterly, while during SIMS weak north westerly are observed. Further, during SMS, winds are strong originating from southwest and moderate north -easterly during FIMS (Fig. 2).

Long-range transport of aerosol has been investigated using Hybrid Single Particle Lagrangian Interpolated Trajectory (HYSPLIT) model (http://ready.arl.noaa.gov/) (Drexler and Rolph, 2003). Five days back trajectories at 500 m and 1500 m have been classified into three distinct source regions namely (a) Continental (b) Maritime and (c) West Asia (Table 2). These heights were chosen to understand the flux of aerosol at the surface and within the planetary boundary layer, which is in the range of 1.5 kms to 2.0 kms (Dharmaraj et al., 2006). Percentage contribution from continental source, maritime source and west Asia are shown in Table 2. Back trajectory revealed that contribution from continental source was the highest during FIMS at both the heights (500 m and at 1500 m). On the other hand least contribution was seen during SIMS and SMS. Upon examining the maritime source, highest contribution was seen during SMS and comparably low (<50%) was observed during WMS and FIMS. West Asian contribution was maximum during SIMS at both the levels. On the other hand negligible (≤ 1) contribution was noticed during SMS and FIMS.

2.2.2. Aerosol optical Depth

Microtops II sunphotometer was used to generate aerosol optical depth (AOD), at five different wavelengths bands centered at 0.380, 0.440, 0.500, 0.675 and 0.870 μm, following a standard protocol (Frouin et al., 2003), on cloud free days from the period January 2008 to December 2010 and seasonal average has been considered in the present study. The instrument computes AOD using internal calibration coefficients and the coordinates of the observation points provided by a Global Position System (GPS) attached to it (Morys et al., 2001). Daily observations were carried out from 0900 to 1730 hrs local time at 30 minutes interval, avoiding the period of obstruction of the sun by passing clouds. Since details on sunphotometer

were given in Menon et al. (2014), the same is not repeated here.

2.3 Methodology

2.3.1.Ångström parameters

Size distribution parameter α is computed using Ångström (1961), following equation (1). It represents the ratio of fine to coarse mode aerosol while β is the turbidity coefficient representing the atmospheric turbidity.

$$\tau = \beta\lambda^{-\alpha} \quad (1)$$

In the present study, α is computed using least square fit of AOD spectra in a log-log scale applying both equation 1 and Volz (1951) method,

$$\alpha = -\frac{d\ln\tau}{d\ln\lambda} - \frac{\ln\left(\frac{\tau_1}{\tau_2}\right)}{\ln\left(\frac{\lambda_1}{\lambda_2}\right)} \quad (2)$$

Where λ1 and λ2 are any pair of wavelengths expressed in μm and τ1 and τ2 are the corresponding AODs.

The range of wavelengths used to estimate α are 0.440 - 0.500 μm and 0.675 – 0.870 μm. In addition, least square fit method was applied to the entire wavelength band 0.440 -0.870 μm.

2.3.2. Second order derivative

The second order polynomial fit to examine the curvature in aerosol spectra can be written as

$$\ln\tau = \alpha 2(\ln\lambda)2 + \alpha 1\ \ln\lambda + \alpha 0 \quad (3)$$

Where α0, α1 and α2 are constants wherein α2 represents the curvature in the spectral curve.

Second order derivative of the Ångström (ά) was derived using Eck et al. (1999) as shown below,

$$\acute{\alpha} = \left(\frac{-2}{\ln\lambda_{i+1} - \ln\lambda_{i-1}}\right)\left(\frac{\ln\tau_{i+1} - \ln\tau_i}{\ln\lambda_{i+1} - \ln\lambda_i} - \frac{\ln\tau_i - \ln\tau_{i-1}}{\ln\lambda_i - \ln\lambda_{i-1}}\right) \quad (4)$$

Using equation (1) and (3),

$$\acute{\alpha} = = -2\alpha_2 \quad (5)$$

Results and discussion

3.1. Spectral variation of AOD

Spectral variation of AOD shows strong wavelength dependence during the study period. In addition the variability exhibits temporal characteristics (Fig. 3). A flat spectra is noticed in the long wavelength during June, August and September (months in SMS), which can be associated with large contribution from coarse mode aerosols, and such large influx of coarse maritime aerosols during the SMS is associated with increased wind speed ,which subsequently enhances the sea-salt generation. On the other hand, steep spectra are observed during rest of the months. Moreover, AOD variability is large, as depicted by large standard deviation, in the shorter wavelength and considerably low standard deviation is observed at longe wavelength. Several studies have been carried out to investigate this fact, and one such study is by Schuster et al. (2006), which established that the fine mode particles have much greater effect on AOD in the visible region. Therefore, such a variability is attributed to aerosol optical properties (Single scattering albedo, asymmetry factor, particle size distribution) (Lyamani et al., 2004; Reid et al., 1999).Variations are more conspicuous at shorter wavelength ($\lambda \leq 0.650\mu m$), wherein submicron aerosol contributes significantly to AOD. These particles are believed to be formed from secondary production mechanism (i.e. gas to particle conversion) and grow by microphysical properties and thus are associated with anthropogenic activities (Ramanathan et al., 2001). On the other hand, the coarse particles which influence the longer wavelength are short lived. Similar observations were made by by various authors (Bhuyan et al., 2005; Moorthy et al., 2007). To analyze these characteristics further, temporal variability of AOD at 0.500 μm (an intermediate wavelength) is presented below.

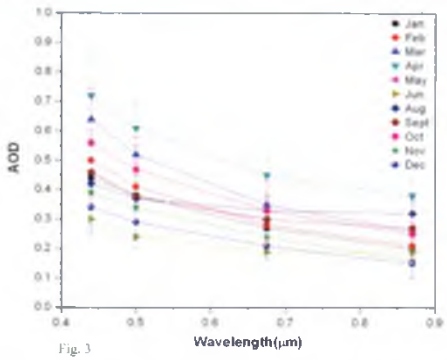

Fig. 3

Fig.3. Mean intraannual spectral variation in AOD over the study area for the period 2008-2010. The vertical bar denotes ±1σ.

3.2. Aerosol optical depth

Seasonal variation in AOD (0.500μm) for the period 2008- 2010 is shown in Figure 4. Highest AOD was observed during SIMS (0.43±0.18) and lowest during SMS (0.32±0.10). During WMS observed AOD was 0.42±0.12 while in FIMS it was 0.39±0.11. In order to understand the inter-annual variability, monthly mean AOD at 0.500 μm during different months from 2008 to 2010 has been analysed. Total number of observations considered for the study was 994, with vertical bars denoting the standard deviation (±1σ). On examining AOD at 0.500 μm, it was found that AOD gradually increased from January (0.38±0.2) reaching a value of 0.41± 0.05 during February followed by 0.52± 0.03 during March. Thereafter AOD attained a peak value of 0.61± 0.08 during April. Further, it was noticed that AOD decreased drastically to 0.37±0.13

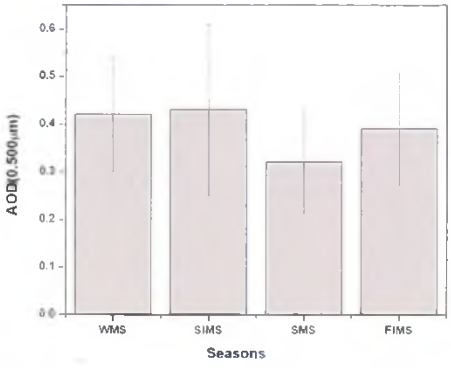

Fig.4. Seasonal mean variation in Aerosol Optical Depth (AOD) at 0.500 μm, during (a) WMS (b) SIMS (c) SMS and (d) FIMS for the period of 2008- 2010.The vertical bars denotes ±1σ.

during May and reached a minimum value during June (0.24±0.04). From August onwards, AOD starts building up gradually from 0.37± 0.08 to 0.38±0.05 during September. Subsequently, it increased to 0.47±0.11 during October and thereafter starts decreasing from 0.34±0.09 in November to 0.29±0.06 in December.

To understand the heterogeneity in aerosols spectral and temporal variation, meteorological factors and air mass back trajectories were analsyed extensively in the present study. During April/May (SIMS), since the local meteorology reveals decrease in influx of continental type of aerosol (wind direction changes from south-southwesterly to west-southwesterly), considerable amount of maritime aerosols are expected over this region. However, back trajectory analysis revealed remarkable results, which exhibit high advection of airmass from west Asia during SIMS. Such a change in air mass type is certainly responsible for rapid buildup of AOD during April (a month in SIMS) over the study region. Long range transport of aerosols from west, contributing mainly dust aerosols have been investigated by Li and Ramanathan 2002, wherein mineral dust transport was found to cross northern Arabian Sea and reach the west coast of India, thus increasing the AOD. Similar build up was investigated in various studies (e.g., Moorthy et al., 1993; Satheesh and Shrinivasan, 2000; Vinoj et al., 2004). However, in tropical region (Latitude < 230N) peak was attained during summer or pre-monsoon months (March, April, May) whereas at higher latitudes (latitude > 230N) the peak was observed during May or June (Bhuyan et al., 2005). For example Ranjan et al. (2007) reported highest AOD during month of July over Rajkot and attributed it to increased vertical mixing , dry surface and windblown dust, whereas Sagar et al. (2004) reported peak AOD during June over a region in central Himalaya, although the magnitude of AOD varies from region to region. An increase in AOD could be due to either of the following factors or due to both 1) decrease in wind speed (increase in residence time of aerosol) and 2) hygroscopic growth due to increase in relative humidity. Analysis revealed that though both the above factors are not favorable during April, AOD increases (Menon et al., 2014).

Another factor attributing to increase in AOD during SIMS is the increased convective activities within the boundary layer which could lead to mixing of aerosols. The meteorological parameters are favorable for such phenomena, i.e heating of land mass and increase in the wind speed, which augment the pumping of aerosol from dry surface. Moreover, in their studies Aloysius et al. (2011) have brought out the significance of vortices and convergences in spatial distribution of aerosol. Coastal aerosols are hygroscopic in nature and hygroscopic growth of particles can occur during period of high relative humidity (Menon et al., 2011). However, Eck et al (2001) suggested that it is not certain that RH reaches significantly high in order for aerosol growth to occur. Interestingly, no clear correlation could be established between AOD and RH in the present case, though there exists one to one corresponding between RH and AOD in some (June, August and September) months. In a typical aerosol model study by Hänel (1976) and Shettle and Fenn, (1979), effect of RH on the growth of particles leading to increase in the mode radii was shown. In this context, Moorthy et al. (1990) in their observational study over Trivandrum found that these results does not hold true entirely. However, some studies focusing on daily variation of AOD have found that diurnal variability of the relative humidity follows that of AOD (Kaskautis et al., 2006, Gerasopoulos et al., 2003).

The study region experiences maximum rainfall during June-September (SMS). Wind speed is particularly high during this season, which gradually increases and peaks to 2.10 m/s and decreases towards the end of September. This period experiences westerly to south-westerly with high relative humidity. In their study Moorthy et al. (1990) reported a weak westerly in the beginning of the season which advances along with the season. Such a strong wind results in sea surf and whitecaps and production of considerable marine aerosols due to surf. Further, these marine aerosols are transported over the coastal regions. Suzuki and Tsunogai, (1998) also reported such transport of marine aerosols over coastal Japan. Same scenario is depicted from the long range transport analysis wherein 95% to 98 % of the air mass type is maritime in nature. This confirms that there is a large influx of marine aerosol over the study region during SMS. Lowest AODs are recorded during this season, nevertheless an increasing trend is seen from June to September wherein the AOD lies between 0.24 and 0.38.The increased rainfall augments the wet removal processes and large particle are removed faster due to gravity (Junge et al., 1955).Thus we conclude that, large wet scavenging reduces AOD drastically, moreover the particles are coarse maritime in nature, thereby enhancing this reduction. Modeling studies by Flossmann et al. (1985) showed that concentration of aerosol particle is reduced by 48% - 94% through the rainout process and

the reduction is mainly confined to larger particles. Similar reduction was noticed by various authors (Moorthy et al., 1990; Paramashewaran et al., 1994; Vinoj et al., 2004; Bhuyan et al., 2005). Observations during the monsoon months are possible only during break period and such days are observed mostly during August and September, June and July experiences extreme rainfall over the study region. Any depletion of aerosols by washout would be replenished atleast partially due to increased production owing to higher wind speed .This could be ascribed as the reason for comparatively higher AOD's during August and September (i.e. from 0.24 in June to ~ 0.38 during August and September).

FIMS is a transition period with considerable amount of rainfall. During FIMS (October and November), mean wind speed reduced almost by 50% of that as observed during SMS, and the synoptic wind is from south-west to north-easterly direction (Fig. 2). Production of marine aerosols became weak due to decrease in wind speed. However, increased AOD is observed during October, which exhibits the secondary peak in AOD, thus making the AOD variation bi-modal. Interestingly, major contribution is from marine source during October, while continental source during November. This increases the complexity of the atmosphere, which is reflected by higher standard deviation during these months. Moreover, as discussed earlier, isolated rains causing washout of aerosol is only a local event and washed aerosols are replenished quickly by the transport of aerosols from surrounding region. Menon et al. (2014), reported that lowest wind speed experienced in October would increase the residence time of aerosol, coupled with development of atmospheric convergence and vortices, increases AOD in October.

During WMS i.e the period from December to March, synoptic wind pattern shows a distinct easterly wind originating from north-east region of Indian subcontinent, such that continental nature of the prevailing airmass is highly conducive for higher aerosol loading. This is clearly reflected with a gradual build up of AOD during WMS. With negligible rainfall (~2% of annual rainfall) and moderate wind speed the atmosphere is conducive for higher aerosol loading. Ramanathan et al (2001) reported that aerosol have their longest residence time during this period making them amenable for long range transport. Similarly, Saha et al. (2005) in their study over Trivandrum, reported a similar increase in AOD during the winter season and attributed it to the lack of wet removable processes. Thus it is established that local meteorological factors in addition to distant sources enhances the AOD loading during WMS over the study region.

3.3. Variability in Ångström parameters (α, β)

Values of alpha $\alpha > 1$ may suggest a large anthropogenic component of submicron particles associated with secondary generation mechanism, while $\alpha < 1$ suggests

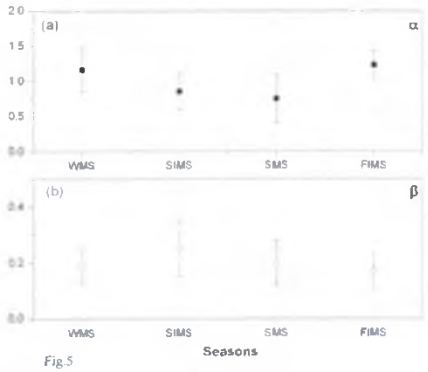

Fig.5

Fig.5. Variability of (a) Ångström exponent (α) and (b) turbidity coefficient β during different season.

influence of larger sea salt/ mineral dust particles or particles grown under high relative humidity (Nakajima et al., 1996; Reid et al., 1999; Eck et al., 1999). Figure 5a represents seasonal mean values of α computed during WMS (n=569), SIMS (n=131), SMS (n=38) and WMS (n=256), in the wavelength range 0.440 – 0.870 μm, applying the least-square methods. Highest α was observed during FIMS which is as high as 1.23 ± 0.19 followed by 1.16±0.32 during WMS. α remains lowest during the SMS (0.75±0.34) whereas it was 0.85±0.25 during SIMS. Higher standard deviation is observed during SMS and WMS. Further, β analysis revealed a contrasting trend, wherein β remained least during FIMS (0.17±0.05) and during WMS (0.19±0.06). On the other hand, highest β is noticed during SIMS (0.25±0.10) followed by SMS (0.20±0.08). As observed from the analysis of both local meteorology and back trajectory, higher α during FIMS and WMS over the present study arises due the increased influx of submicron continental type aerosols, whereas lower α during SMS is due to the fact that the environment is governed predominantly by coarse maritime aerosols during southwest monsoon. Further, β is higher during SIMS, which may be due to the large contribution from dust aerosols from west Asia. However, the variability of β is found to be less conspicuous as compared to that of α (Fig. 5b). Higher α during post-monsoon and winter season whereas comparatively lower values during monsoon and pre-monsoon season , coupled with lower β during post-monsoon and winter while higher during monsoon and pre-monsoon are reported by various authors. Table 3 represents α and β computed over different regions of the Indian subcontinent .Thus, it is clear that high α (>1) are consistent feature over most of the Indian landmass during WMS and FIMS, however local variation are expected depending upon region specific nature of the site (e.g industrial/urban/ coastal / arid).

3.4. Wavelength dependence of AOD

Ångström exponent α, expresses the wavelength dependence of AOD and it is expected that different aerosol type affect its spectral behavior (O' Neill et al., 2001, 2002). This

made authors to determine α from different spectral bands. Different α values were determined in different spectral bands by various authors (Eck et al 1999; Reid et al 1999). Schuster et al. (2006) suggested determination of α in short (0.400 - 0.500μm) and long (0.675 - 0.870 μm) wavelength spectral regions, which can provide information on type of aerosols dominating the region. In this context AOD's at 0.500 μm during different seasons are correlated with α computed at short (α0.440-0.500), long (α0.675- 0.870) and whole (α0.440-0.870) wavelength regions (Fig. 6). The large spread at short as well as long wavelength regions arises due to low turbid condition i.e. at lower AOD's. This feature is observed in present case during all the seasons. However, it is interesting to note that this feature is strong in the shorter wavelength region as compared to long wavelength region. It is observed that in general α 0.440-0.500 shows a decreasing trend during SIMS, SMS and FIMS and increasing trend during WMS. While α0.675-0.870 shows an increasing trend during WMS and SMS, decreasing trend during FIMS and a neutral trend during SIMS. Further, α0.440-0.870 shows almost a neutral trend during SIMS and SMS, while increasing during WMS and decreasing during FIMS. With weak correlation between α0.440-0.870 and AOD at 0.500μm, during SIMS and SMS, it is established that the atmosphere consists of mixed aerosol type. α0.670-0.870 exhibit higher values under turbid conditions, which is also evident in the present study where α0.670-0.870 remains greater than zero almost for all data during SIMS and as discussed earlier, this season experiences high aerosol load.

Ångström equation does not fit the data points exactly, but a second order polynomial fit to lnAOD versus lnλ data provides excellent agreement with measured AOD, resulting in an uncertainty in the measurement with the difference of the order of ~0.01 – 0.02, while a liner fit yields significant differences with measured AOD (Kaskaoutis et

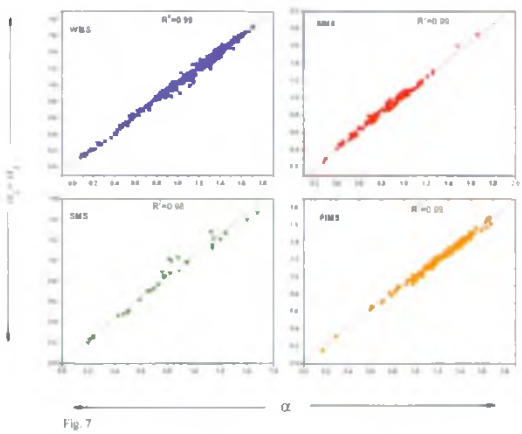

Fig. 7

Fig.7. Correlation between Ångström exponent α and difference in the coefficient of the polynomial fit (α2- α1) during different season.

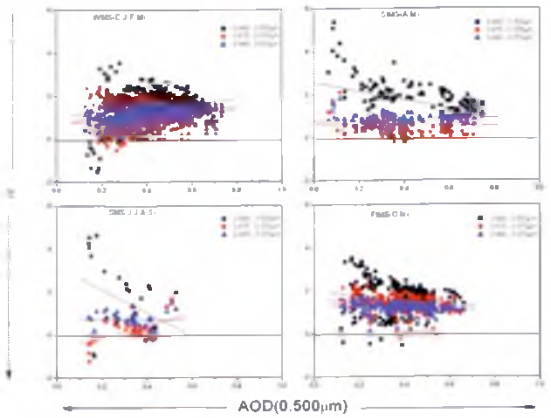

Fig. 6

Fig.6. Correlation between AOD (0.500 μm) and α computed at short (α0.440-0.500), long (α0.675- 0.870) and whole (α0.440-0.870) wavelength region during (a) WMS (b) SIMS (c) SMS and (d) FIMS.

al 2006; Eck et al 1999, 2001; O'Neill et al., 2001). Eck et al. (1999), proposed second order derivative of ln τ versus ln λ so as to quantify the curvature of the AOD spectra .The second order derivative is a measure of the rate of change of the slope with respect to wavelength and thus is a logical complement to the Angstrom exponent, which is the negative of the slope (first derivative) of ln τ versus ln λ.

It is well established fact that the curvature effect in the spectral distribution of AOD's are better quantified by deriving second order Angstrom exponent ά and by fitting a second order polynomial to the measured AOD spectra. Positive values of ά are characteristic of fine mode aerosol dominating the aerosol size distribution (Biomass or urban /industrialized), while ~0 or negative values of ά, implies dominance of coarse mode aerosol in the size distribution curve (Eck et al., 1999; O'Neill et al., 2001).In this context, ά is investigated over the study area and the percentage during different seasons is presented in Table 4. It is observed that percentage of the positive ά decreased from 25% during WMS to 9% during SIMS. Further, during SMS it is found to decrease to 8%, however towards FIMS a drastic increase to 49% is noticed. Negative percentage of the ά value shows an opposite trend, wherein higher percentage is observed during SMS (~92%) and SIMS (89%).

The coefficient of the polynomial fit (α1 and α2) can be used to get significant information about aerosol type in a multimodal aerosol size distribution curve. Schuster et al. (2006) pointed out that to a first approximation, α can be computed from difference between α2 and α1, this is due to the fact that when the curvature is negligible in the AOD spectra, i.e. when α2 is ~0 then α=- α1 following Angstrom power law equation and second order polynomial fit

equation , which would result $\alpha = \alpha 2 - \alpha 1$.Schuster et al. (2006), further revealed that AOD spectra for which $\alpha 2 - \alpha 1 \geq 2$ shows dominance of fine mode aerosol while $\alpha 2 - \alpha 1 \leq 1$ shows dominance of coarse mode aerosols, while values between 1 to 2 represent mixture mode environment or fine mode.

To investigate this over the present study, correlation between α and $\alpha 2 - \alpha 1$ has been plotted (Fig. 7). It is observed that the correlation between these two parameters is strong during all the seasons with R2 value varying between 0.98 and 0.99. Kedia et al. (2011) showed a similar tend and pointed out the validity of $\alpha 2 - \alpha 1 = \alpha$. Further Table 4 shows the percentage of $\alpha 2 - \alpha 1$ computed in above described group i.e. $\alpha 2 - \alpha 1 \leq 1$, $\alpha 2 - \alpha 1 \geq 2$ and $1 < \alpha 2 - \alpha 1 < 2$. It is observed that FIMS shows high percentage of $1 < \alpha 2 - \alpha 1 < 2$, i.e. 92% thereby indicating that the aerosol size distribution spectra is dominated by either by wide range of fine mode aerosol or mixture of modes. Moreover SMS shows higher (89%) $\alpha 2 - \alpha 1 \leq 1$, thus confirming the presence of coarse mode of particle in the size distribution spectrum. Interestingly not much dominant contribution from fine mode aerosol was noticed, although WMS showed ~15% which is highest among all the season.

4. Conclusions

AOD is analyzed for the period 2008-2010 over a coastal site in Goa, the following preliminary conclusions are drawn from the present study:

(1) Seasonal variability shows highest AOD during SIMS (0.43), which is associated with considerable influx of aerosol from west Asia. On the other hand lowest is seen during SMS (0.32), wherein extensive rainfall, responsible for wet removal process thereby reduces AOD. Interannual variability shows a primary peak during April and a secondary peak during October. Significant buildup of AOD is noticed from December to March, associated with increasing continental air mass flux. Further, spectral dependence is vivid from near flat spectra during June, August and September, indicating dominance of coarse mode aerosols.

(2) Large seasonal variability is observed in the Ångström parameters, α and β. Ångström exponent α, is found to be high during FIMS (1.23) and WMS (1.15), indicating the dominance of finer mode aerosols. On the other hand low value of 0.74 during SMS, revealed the coarse mode aerosol type. Variation in β, are less conspicuous, however highest β is observed during SIMS (0.25), thus indicating higher columnar loading during SIMS.

(3) α computed at shortwave (α0.440-0.500), longwave (α0.675- 0.870) and entire(α0.440-0.870) spectrum, revealed different values in different wavelength region. Correlation between AOD (0.500μm) a id in different wavelength region showed varing tr nd during different seasons. Neutral trend betv ee AOD (0. 500μm) and α 0.440-0.870 during SiMS and SMS shows a bimodal aerosol size distribution

(4) Second order Ångström exponent á, shows highe percentage of á which is negative or ~ zero, durin SIMS (89%) and SMS (92%), thus indicatin aerosol size distribution with dominant coars mode or a bimodal distribution with coarse mod particles. However, higher percentage of positive á value is noticed during FIMS (49%), depicting higher fine mode aerosols dominating the size distribution.

(5) Difference between the coefficients of polynomial fit ($\alpha 2 - \alpha 1$), reveal that large percentage of $\alpha 2 - \alpha 1$ are ≤ 1 during SMS (89%) confirming the presence of coarse mode aerosols in the size distribution. Moreover ~92% of $\alpha 2 - \alpha 1$ are observed between 1 and 2, thus during FIMS, showing that a wide range of fine-mode fraction or mixture modes prevail over the study region.

Acknowledgement

The authors like to acknowledge NIO, Goa and IMD Goa, for providing necessary meteorological data. They also wish to thank Dr. K. Krishnamoorthy for providing funding under Aerosol Radiative Forcing (ARFI) of Indian Space Research Organization (ISRO). The authors also wish to thank Vice Chancellor of Goa University for all the facilities extended to carry out the work. This is a contribution under ARFI project.

References

Alosius, M., Sijikumar, S., Prijith, S.S., Mohan, M., Parameshwaran, K., 2011. Role of dynamics in the advection of aerosol over the Arabian Sea along the west coast of peninsular India during pre-monsoon season: A case study based on satellite data and regional climate model. Journal of Earth System Science 120, 269–279.

Ångström, A., 1961. Techniques of determining the turbidity of the atmosphere. Tellus 1961; 13: 214-23.

Babu, S.S., Satheesh, S.K., Moorthy, K.K., 2002. Aerosol radiative forcing due to enhanced black carbon at an urban site in India. Geophysical Research Letters 29(18), 1880. doi:10.1029/2002GL015826.

Beegum, N.S., Moorthy, K.K., Babu, S.S., 2009. Aerosol microphysics over a tropical coastal station inferred from the spectral dependence of Ångström wavelength exponent and inversion of spectral aerosol optical depths. Journal of Atmospheric and Solar-Terrestrial Physics 71, 1846–1857. doi:10.1016/j.jastp.2009.07.004.

Bhuyan, P.K., Gogoi, M.M., Moorthy, K.K., 2005. Spectral and temporal characteristics of aerosol optical depth over a wet tropical location in northeast India. Advances in Space Research 35, 1423–1429.

Charlson, R.J., Schwartz, S.E., Hales, J.M., Cess, R.D., Coakley Jr., J.A., Hansen, J.E., Hofmann, D.J., 1992. Climate forcing by anthropogenic aerosols. Science 255, 423–430.

Dharmaraj, T., Murthy, B,S., Sivaramakrishnan, S., 2006. Vertical structure of the lower atmosphere over the Arabian Sea and the west coast station during weak phase of the Indian summer monsoon. Indian Journal of Radio and Space Physics 35, 418–423.

Draxler, R., Hess, G.D., 1998. An overview of the HYSPLIT-4 modeling system for trajectories, dispersion and deposition. Australian Meteorological Magazine 47, 295–308.

Eck, T.F., et al., 1999. Wavelength dependence of the optical depth of biomass burning, urban, and desert dust aerosols. Journal of Geophysical Research 104 (D24). doi:10.1029/1999JD900923.

Eck, T.F., Holben, B.N., Dubovic, O., Smirnov, A., Slutsker, I., Lobert, J.M., Ramanathan, V., 2001. Column-integrated aerosol optical properties over the Maldives during the northeast monsoon for 1998-2000. Journal of Geophysical Research 106, 28555–28566.

Flossmann, A.I., Hall, W.D., Pruppacher, H.R., 1985. A theoretical study of the wet removal of atmospheric pollutant – Part I: The redistribution of aerosol particles captured through nucleation and impaction scavenging by growing cloud drops. Journal of Atmospheric Sciences 42, 441–463.

Frouin, R., Holben, B., Miller, M., Pietras, C., Kirk, K.D., Fargion, G.S., Porter, J., Voss, K., 2003. Sun and sky radiance measurements and data analysis protocols. In: Mueller, J.L., Fargion, G.S., MacClain, C.R. (Eds.), Ocean Optical protocols for Satellite Ocean Color Sensor Validation, Revision 4, radiometric measurements and data analysis protocols, NASA/TM-2003-211621/Rev4-Vol-III, Vol-III. NASA, Goddard Space Flight Center, Greenbelt, MA, pp. 60–69.

Gerasopoulos, E., Andreae, M.O., Zerefos, C.S., Andreae, T.W., Balis, D., Formenti, P., Merlet, P., Amiridis, V., Parastefanou, C., 2003. Climatological aspects of aerosol optical properties in Northern Greece. Atmospheric Chemistry and Physics 3, 2025–2041.

Guleria, R.P., Kuniyal, J.C.,Dhyani P.P., 2012. Seasonal variability in aerosol optical and physical characteristics estimated using the application of the Angstrom formula over Mohal in the northwestern Himalaya. India Journal of Earth System Science 121, 697– 710.

Hänel, G., 1976. The properties of atmospheric aerosol particles as functions of relative humidity at thermodynamic equilibrium with surrounding moist air. In: Advances in Geophysics, vol. 19. Academic Press, New York, pp. 73–188.

IPCC, 2007. In: Solomon, S., Qin, D., Manning, M., Chen, Z., Marquis, M., Averyt, K.B., Tignor, M., Miller, H.L., (Eds.), Summary for Policymakers. In: Climate Change 2007: ThePhysical Science basis. Contribution of Working Group I to the Fourth Assessment Report of the Intergovernmental Panel on Climate Change. Cambridge University Press, Cambridge, United Kingdom and New York, NY, USA.

Junge, C. E., 1955. The size distribution and aging of natural aerosols as determined from electrical and optical measurements in the atmosphere. Journal of Meteorology 12, 13–25.

Kaskaoutis, D.G., Kharol, S.K., Sinha, P.R., Singh, R.P., Badarinath, K.V.S., Mehdi, W., Sharma, M., 2011. Contrasting aerosol trends over South Asia during the last decade based on MODIS observations. Atmospheric Measurements Techniques Discussion 4, 5275–5323.

Kedia, S., Ramachandran, S., 2009. Variability in aerosol optical and physical characteristics over the Bay of Bengal and the Arabian Sea deduced from Ångström exponents. Journal of Geophysical Research 114 (D14207). doi:10.1029/2009JD011950.

Kedia, S., Ramachandran, S., 2011. Seasonal variation in aerosol characteristics over an urban location and a remote site in western India. Atmospheric Environment 45. doi:10.1016/j.atmosenv.2011.01.040.

Li, F., Ramanathan, V., 2002. Winter to summer variation of aerosol optical depth over the tropical Indian ocean. Journal of Geophysical Research 107 AAC 2, 1–13.

Madhavan, B.L., Niranjan, K., Sreekanth, V., Sarin, M.M., Sudheer, A.K., 2008. Aerosol characterization during the summer monsoon period over a tropical coastal station, Viskhapatanam. Journal of Geophusical Research 113 (D21208).

Menon, H.B., Shirodkar, S., Kedia, S., Ramachandran, S., Babu, S.S., Moorthy, K.K., 2014. Temporal variation of aerosol optical depth and associated shortwave radiative forcing over a coastal site along the west coast of India. Science of the Total Environment 468-469. doi:org/10.1016/j.scitotenv.2013.08.013.

Moorthy, K.K., Babu, S.S., Satheesh, S.K., 2003. Aerosol spectral optical depths over Bay of Bengal: Role of transport. Geophysical Research Letters 30, 1249. doi:10.1029/2002GL016520.

Moorthy, K.K., Babu, S.S., Satheesh, S.K., 2005. Aerosol characteristics and radiative impacts over Arabian Sea during inter-monsoon season: Results from ARMEX field campaign. Journal of Atmospheric Sciences 62, 192–206.

Moorthy, K.K., Babu, S.S., Satheesh, S.K., 2007. Temporal heterogeneity in aerosol characteristics and the resulting radiative impact at a tropical coastal station-I: Microphysical and optical properties. Annales Geophysicae 25, 2293–2308.

Moorthy, K.K., Nair, P.R., Murthy, B.V.K., 1990. Size distribution of Coastal Aerosols: Effect of Local Sources and Sinks. Journal of Applied Meteorology 30, 844–852.

Morys, M., Mims III, F.M., Hagerup, S., Anderson, S.E., Baker, A., Kia, J., Walkup, T., 2001. Design, calibration, and performance of Microtops II handheld ozone monitor and Sun photometer, Journal Geophysical Research. 106, 14,573–14,582.

Nakajima, T., Glauco, T., Rao, R., Kaufman, Y.J., Holben, B.N., 1996. Use of sky brightness measurements from ground for remote sensing of particulate polydispersions. Applied Optics 35, 2672–2686.

O'Neill, N.T., Eck, T.F., Holben, B.N., Smirnov, A., Dubovic, O., 2001. Bimodal size distribution influences on the variation of Ångström derivates in spectral and optical depth space. Journal of Geophysical Research 106 (D9), 9787–9806.

O'Neill, N.T., Eck, T.F., Holben, B.N., Smirnov, A., Royer, A., Li, Z., 2002. Optical properties of boreal forest fire smoke derived from Sun photometry. Journal of Geophysical Research 107, D11.

Parameshwaran, K., Vijaykumar, G., Murthy, B.V. K., Moorthy, K.K., 1994. Effect of wind speed on Mixing Region Aerosol Concentrations at a Tropical Coastal Station. Journal of Applied Meteorology 34, 1392–1397.

Ramachandran, S., 2004. Spectral aerosols characteristics during the northeast monsoon over the Arbain Sea and the tropicl Indian Ocean: Angstrom parameters and anthropogenic influence. Journal of Geophysical Research 109 (D19208). doi:10.1029/2003JD004483.

Ramanathan, V., Crutzen, P.J., Kiehl, J.T., Rosenfeld, 2001. Aerosol, Climate and Hydrological cycle. Science 294, 2119–2124.

Ranjan, R.R., Joshi, H.P., Iyer, K.N., 2007. Spectral variation of total column aerosol optical depth over Rajkot: A Tropical semi-arid Indian station. Aerosol and Air Quality Research 7 no.1, 33–45.

Reid, J.S., Eck, T.F., Christopher, S.A., Hobbs, P.V., Holben, B.N., 1999. Use of the Ångström exponent to estimate the variability of optical and physical properties of aging smoke particles in Brazil. Journal of Geophysical Research 104 (D22), 27473–27489.

Sagar, R., Kumar, B., Dumka, U.C., Moorthy, K.K., Pant, P., 2004. Characteristics of aerosol spectral optical depths over Manora Peak: A high – altitude station in the central Himalayas. Journal of Geophysical Research 109 (D06207).

Saha, A., Moorthy, K.K., 2005. Interannual variation of aerosol optical depth over coastal India: Relation to synoptic meteorology. Journal of Applied Meteorology 44, 1066–1077.

Satheesh, S.K., Moorthy, K.K., Das, I., 2001. Aerosol spectral optical depths over Bay of Bengal, Indian Ocean, and Arabian Sea. Current Science 81, 1617–1625.

Satheesh, S.K., Srinivasan, J., 2002. Enhanced aerosol loading over Arabian Sea during the pre-monsoon season: Natural or anthropogenic? Geophysical Research Letters 29. doi:10.1029/2002GL015687.

Schuster, G.L., Dubovik, O., Holben, B.N., 2006. Angstrom exponent and bimodal aerosol size distributions. Journal of Geophysical Research 111 (D07207). doi:10.1029/2005JD006328.

Shettle, E.P., Fenn, R.W., 1979. Models for the aerosols of the lower atmosphere and the effect of humidity variation on their optical properties. AFGK-TR-079-0214.

Singh, R.P., Dey, S., Tripathi, S.N., Tare, V., 2004. Variability of aerosol parameters over Kanpur, northern India. Journal of Geophysical Research 109 (D23206).

Suresh, T., Desa, Elgar., 2005. Seasonal variation of aerosol over Dona Paula, a coastal site on the west coast of India. Atmospheric Environment 39, 3471–3480.

Suzuki, T., Tsunogai, S., 1988. Daily variation of aerosols of marine and continental origin in the surface air over a small island Okushiri in the Japan Sea. Tellus 40B, 42-49.

Vinoj, V., Satheesh, S.K., 2003. Measurements of aerosol optical depth over Arabian Sea during summer monsoon season. Geophysical Research Letters 30(5), 1263. doi:10.1029/2002GL016664.

Vinoj, V., Satheesh, S.K., Babu, S.S., Moorthy, K.K., 2004. Large aerosol optical depths observed at an urban location in southern India associated with rain–deficit summer monsoon season. Annales Geophysicae 22, 3073-3077.

Volz, F., 1959. Photometer mit Selen-photoelement zur spektralen Messung der Soennestrahlung und zur Bestimmung der Wallenlangeabhangigkeit der Dunstrubung. Archiv fur Meteorologie Geophysik und Bioklimatologie 10, 100–131.

Table.1. Seasonal mean variation of meteorological parameters during WMS, SIMS, SMS and FIMS for the period of 2008- 2010.

Meteorological parameters	WMS(D,J,F,M)	SIMS(A,M)	SMS(J,J,A,S)	FIMS(O,N)
Wind speed(m/s)	1.09±0.07	1.37±0.02	2.10±0.45	1.00±0.11
Wind Direction (deg)	171±14.91	232±2.70	226±6.95	153±3.42
Relative Humidity (%)	70±1.13	73±2.11	88±5.2	80±9.7
Rainfall (mm)	17±22.22	30±33.10	725±106	161±138

Table.2. Percentage contribution of air mass back trajectory at 500m and 1500m over the study area. The air mass trajectory from northwest India crossing central and east coast of India, from central India and from northeast India represents continental source. Area crossing Bay of Bengal, Arabian Sea and west coast of India represents maritime source. Trajectories originating from Arabian peninsula crossing Arabian Sea and northwest India are identified and termed as West Asia.

Season	Continental		Maritime		West Asia	
Heights	500 m	1500m	500 m	1500m	500 m	1500m
WMS	49	52	37	41	14	7
SIMS	1	20	78	56	22	24
SMS	2	4	98	95	0	1
FIMS	56	68	44	31	0	1

Table.3.Season wise variation of Ångström exponent (α) and turbidity coefficient β over Indian Subcontinent and adjoining Sea.

Seasons	Location	α	β	Reference
WMS	Vishakapatnam	1.08±0.03	0.19	Ramachandran 2004
	Trivandrum	1.0±0.08	0.17	Ramachandran, 2004
	Port Blair	1.24	0.14	Moorthy et al. 2003
	Coastal India	1.49±0.10	0.14	Ramachandran 2004
	Bay of Bengal	1.23±0.43	0.20	Satheesh et al. 2001
SIMS	Bangalore	1.30±0.01	0.13	Moorthy et al. 2005
	Kanpur	0.60±0.31		Singh et al. 2004
	Arabian Sea	1.17±0.03	0.21	Moorthy et al 2005
	TVM	0.85±0.04	0.22	Moorthy et al. 2007
SMS	Kanpur	0.66±0.45		Singh et al. 2004
	Dibrugarh	0.6		Bhuyan et al. 2005
	Arabian Sea	0.35±0.12	0.36	Vinoj and Satheesh 2003
	TVM	0.32±0.02	0.25	Moorthy et al. 2007
FIMS	Bangalore	1.06±0.02	0.12	Babu et al. (2002)
	Kanpur	1.12±0.28		Singh et al. (2004)
	TVM	1.20±.01	0.16	Moorthy et al. 2007

Table.4. Percentage representation of seasonal mean variation in positive and negative values of second order Ångström exponent á and coefficient of the polynomial fit (α1 and α2) grouped into α2- α1 ≤ 1 , 1 < α2- α1 < 2 and α2- α1 ≥ 2 during different seasons.

Season	Positive á	Negative á or ~ zero	α2- α1 ≤ 1	1 < α2- α1 < 2	α2- α1 ≥ 2
WMS	25	73	11	74	15
SIMS	9	89	60	38	2
SMS	8	92	89	11	0
FIMS	49	51	4	92	4

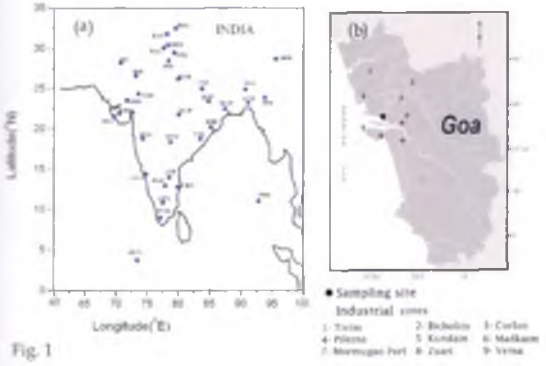

Fig.1 (a) Network of stations under the Aerosol Radiative Forcing over India (ARFI) project (b) ARFI station at Goa, different industrial zones are shown as numbers from 1 to 9.

phenomenon within the boundary layer. Several industrial sites are located in the proximity of the sampling site and closest among all is the Murmagao port (Fig. 1b). Ore produced as an outcome of mining, which is a significant activity in Goa, is transported to Murmagao port mainly through Mandovi and Zuari rivers.

2.2. In-situ measurements

2.2.1. Meteorological factors

Aerosol spatial and temporal variability are governed by meteorological factors and the parameters were measured using automatic weather station (AWS). Rainfall data for the study period was obtained from Indian meteorological department situated ~4 kms from the study site. Seasonal mean variation of the meteorological factors is shown in Table 1. Wind speed increased from 1.09 m/s in WMS to 1.37 m/s in SIMS and attaining a peak of 2.10 m/s during SMS, further it reduces to 1 m/s during FIMS. It is observed that winds are mostly south/ southeasterly during WMS and southwesterly during SIMS. During SMS, wind direction changes entirely to westerly which attains southeasterly during FIMS. Relative humidity shows an increasing trend from WMS till SMS, thereafter decreases as FIMS approaches. SMS receives above normal rainfall over the study region where rainfall of 725 mm is recorded. Considerable amount of precipitation is also seen during FIMS (161mm), which is a transition phase. Rainfall during April/May constitutes to a seasonal mean of 30 mm of precipitation. Negligible amount of precipitation is noticed in December during WMS (~17 mm).

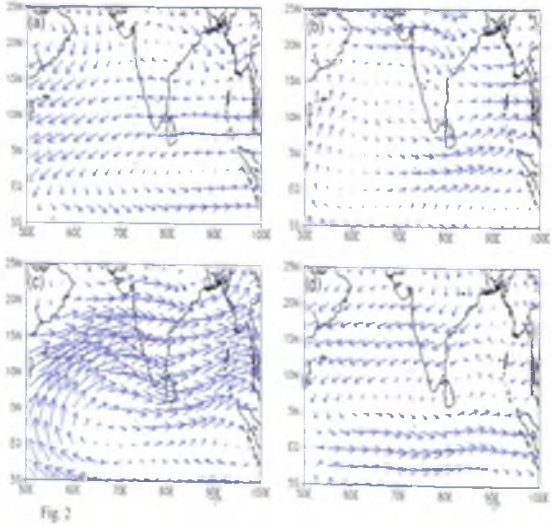

Fig.2. Synoptic wind (m/s at 850 hPa) over India during (a) WMS (b) SIMS (c) SMS and (d) FIMS.

Synoptic wind at surface (850 hPa), using National Center for Prediction (NCEP) data, revealed that during WMS, winds are moderate and easterly, while during SIMS weak north westerly are observed. Further, during SMS, winds are strong originating from southwest and moderate north –easterly during FIMS (Fig. 2).

Long-range transport of aerosol has been investigated using Hybrid Single Particle Lagrangian Interpolated Trajectory (HYSPLIT) model (http://ready.arl.noaa.gov/) (Drexler and Rolph, 2003). Five days back trajectories at 500 m and 1500 m have been classified into three distinct source regions namely (a) Continental (b) Maritime and (c) West Asia (Table 2). These heights were chosen to understand the flux of aerosol at the surface and within the planetary boundary layer, which is in the range of 1.5 kms to 2.0 kms (Dharmaraj et al., 2006). Percentage contribution from continental source, maritime source and west Asia are shown in Table 2. Back trajectory revealed that contribution from continental source was the highest during FIMS at both the heights (500 m and at 1500 m). On the other hand least contribution was seen during SIMS and SMS. Upon examining the maritime source, highest contribution was seen during SMS and comparably low (<50%) was observed during WMS and FIMS. West Asian contribution was maximum during SIMS at both the levels. On the other hand negligible (≤ 1) contribution was noticed during SMS and FIMS.

2.2.2. Aerosol optical Depth

Microtops II sunphotometer was used to generate aerosol optical depth (AOD), at five different wavelengths bands centered at 0.380, 0.440, 0.500, 0.675 and 0.870 μm, following a standard protocol (Frouin et al., 2003), on cloud free days from the period January 2008 to December 2010 and seasonal average has been considered in the present study. The instrument computes AOD using internal calibration coefficients and the coordinates of the observation points provided by a Global Position System (GPS) attached to it (Morys et al., 2001). Daily observations were carried out from 0900 to 1730 hrs local time at 30 minutes interval, avoiding the period of obstruction of the sun by passing clouds. Since details on sunphotometer